CORTEX 97 (2017) 60–69

Available online at www.sciencedirect.com

ScienceDirect

Journal homepage: www.elsevier.com/locate/cortex

Research report

Task-evoked pupil dilation and BOLD variance as indicators of locus coeruleus dysfunction

Jeremy A. Elman [a,b,*], *Matthew S. Panizzon* [a,b], *Donald J. Hagler Jr.* [c], *Lisa T. Eyler* [a,d], *Eric L. Granholm* [a,d], *Christine Fennema-Notestine* [a,c], *Michael J. Lyons* [e], *Linda K. McEvoy* [c], *Carol E. Franz* [a,b], *Anders M. Dale* [c,f] *and William S. Kremen* [a,b,d]

[a] *Department of Psychiatry, University of California, San Diego, CA, USA*
[b] *Center for Behavior Genetics of Aging, University of California, San Diego, CA, USA*
[c] *Department of Radiology, University of California, San Diego, CA, USA*
[d] *VA San Diego Health Care System, San Diego, CA 92161, USA*
[e] *Department of Psychological and Brain Sciences, Boston University, Boston, MA, USA*
[f] *Department of Neurosciences, University of California, San Diego, CA, USA*

ARTICLE INFO

Article history:
Received 8 May 2017
Reviewed 28 June 2017
Revised 4 August 2017
Accepted 28 September 2017
Action editor Brad Dickerson
Published online 7 October 2017

Keywords:
Pupillometry
Resting-state fMRI
Locus coeruleus
Alzheimer's disease
Ventral attention network

ABSTRACT

Pupillary responses during cognitive tasks are linked to functioning of the locus coeruleus (LC). The LC is an early site of abnormal tau deposition, which may contribute to key aspects of Alzheimer's disease (AD) pathophysiology. We previously found attenuation of pupillary responses to increases in cognitive load in individuals with mild cognitive impairment (MCI), suggesting pupillary responses may provide a biomarker of early risk for AD associated with LC dysfunction. The LC modulates cortical activity through two modes of operation: tonic and phasic. Early LC damage has been predicted to result in a state of persistent high tonic LC activity that may disrupt task-related phasic activity. To further examine whether pupillary responses are associated with early LC dysfunction, we measured pupil dilation during a digit span task as a measure of phasic activity, and low frequency BOLD variance (LFBV) during resting-state fMRI in key nodes of the ventral attention network (VAN) as a measure of cortical reactivity related to LC tonic activity in 358 middle-aged men. Individuals with greater LFBV in VAN nodes, i.e., higher tonic brain activity at rest, showed a smaller increase in pupil dilation from low to moderate cognitive loads. Thus, higher tonic LFBV activity at rest was related to reduced task-appropriate phasic dilation increases. The results support predictions from prominent models of LC functioning in which early LC dysfunction leads to persistent high tonic rates of activity during rest and lower signal-to-noise of phasic responses during task performance. Taken together with previous findings of early AD pathophysiology in LC and reduced phasic dilation responses to increased cognitive load in individuals with MCI, the present results suggest that pupillary responses may index early LC dysfunction and should receive further study as a potential biomarker of risk for AD.

* *Corresponding author*. Department of Psychiatry, University of California, San Diego, 9500 Gilman Dr. (MC0738), La Jolla, CA, 92093, USA.
E-mail address: jaelman@ucsd.edu (J.A. Elman).
https://doi.org/10.1016/j.cortex.2017.09.025

1. Introduction

Increasing evidence suggests that the pathological processes underlying Alzheimer's disease (AD) begin years, if not decades, prior to the onset of behavioral symptoms (Aizenstein et al., 2008; Bateman et al., 2012; Bennett et al., 2006; Jansen et al., 2015). With this knowledge, a shift toward secondary prevention strategies is underway in which intervention is initiated during this extended prodromal state (Dubois et al., 2014; Golde, Schneider, & Koo, 2011; Sperling et al., 2011). There is a great need for early screening tools that are easily implemented, cost effective and come with a relatively low subject burden to enable more widespread use. Pupil dilation measured during a cognitive task may be one such tool. Individuals show increasing pupil dilation that scales with task load until cognitive capacity is exceeded, at which point there is an abrupt decline in pupil dilation (Geva, Zivan, Warsha, & Olchik, 2013; Granholm, Asarnow, Sarkin, & Dykes, 1996).

We previously found differences in pupillary responses recorded during a digit span task in late middle-aged adults based on individual differences in cognitive ability and mild cognitive impairment (MCI), a state presumed to reflect prodromal AD (Granholm et al., 2017). The digit span task elicits a well-characterized pupil dilation response that can be examined for load-dependent changes (Granholm et al., 1996). Individuals with lower capacity (shorter maximum spans) exhibited greater pupil dilation (i.e., required more effort) at lower loads (3- and 6-digit spans) but they had a more marked decrease in dilation at high loads when capacity was exceeded. Individuals with single-domain amnestic MCI, who performed similarly to cognitively normal participants, showed greater compensatory effort (i.e., greater dilation) at lower loads. In contrast, individuals with multi-domain MCI (mMCI), who performed worse than the other groups, demonstrated a flat dilation profile in which phasic cognitive effort did not differ across loads, suggesting that compensatory mechanisms had been overwhelmed even at low loads. However, the neural mechanisms underlying these differences remain unclear.

Additional motivation for the utility of pupil dilation measurements in the study of MCI and early AD comes from findings that the pupil dilation is tightly coupled with activity in the locus coeruleus (LC) norepinephrine (NE) pathways (Alnaes et al., 2014; Gilzenrat, Nieuwenhuis, Jepma, & Cohen, 2010; Koss, 1986; Murphy, O'Connell, O'Sullivan, Robertson, & Balsters, 2014; Rajkowski, Kubiak, & Aston-Jones, 1993; Rajkowski, Kubiak, & Aston-Jones, 1994). Both pupil dilation and activation of noradrenergic neurons in the LC have been shown to increase in a correlated manner with mental (or cognitive) effort (Varazzani, San-Galli, Gilardeau, & Bouret, 2015), and there is evidence of a causal, although potentially indirect, relationship of LC activation with pupil dilation (Joshi, Li, Kalwani, & Gold, 2016). Dysfunction in the LC is relevant to the study of AD because recent disease models suggest that the LC is the earliest site of tau deposits, which may appear prior to age 30 (Braak & Del Tredici, 2011, 2012; although see; Crary et al., 2014). Indeed, deposits of neurofibrillary tangles and extensive tissue loss occur in the LC and have been found to correlate with disease duration and symptom severity (Bondareff et al., 1987; German, White, & Sparkman, 1987, 1992; Grudzien et al., 2007). Our previous findings link differences in pupil dilation to MCI, which is thought to represent an early stage of AD. The current study attempts to further link differences in pupil dilation to dysfunction in the LC, a structure affected by AD pathology early in the disease course.

In order to provide converging evidence that differences in pupil dilation reflect dysfunction in the LC, we were particularly interested in whether an altered pupil response would be associated with changes in cortical activity measured by fMRI, since both may be related to LC functioning and are found to be disrupted in preclinical AD (Ewers, Sperling, Klunk, Weiner, & Hampel, 2011; Granholm et al., 2017; Sperling et al., 2011). Converging evidence suggests that the LC-NE system plays a major role in modulating neural activity in the ventral attention network (VAN) (Corbetta, Patel, & Shulman, 2008; Coull, Büchel, Friston, & Frith, 1999; Dosenbach et al., 2006; Geva et al., 2013; Sara, 2009; Sara & Bouret, 2012). The VAN is a right-lateralized network and includes the right temporoparietal junction (TPJ), anterior cingulate cortex (ACC), and inferior prefrontal cortex (iPFC). The ACC and iPFC have highly recurrent connections with the LC, and the LC modulates task focus through its ability to drive activity within the TPJ (Aston-Jones & Cohen, 2005; Aston-Jones et al., 2002; Samuels & Szabadi, 2008; Walz et al., 2013). During normal functioning, fMRI activity in the VAN is correlated with activity in the LC as well as with pupillary responses (Alnaes et al., 2014; Murphy et al., 2014; Raizada & Poldrack, 2007).

According to the adaptive gain theory (Aston-Jones & Cohen, 2005), an influential model of LC function, the LC modulates neural activity and behavior through two modes of functioning: tonic and phasic. Increased tonic activity facilitates exploration by boosting the gain of VAN neurons, increasing their baseline firing rate. In contrast, the phasic mode facilitates task performance by increasing the signal-to-noise ratio, suppressing responses to irrelevant stimuli while allowing evoked responses to task-relevant stimuli (Aston-Jones & Cohen, 2005; Corbetta et al., 2008; Sara & Bouret, 2012).

To examine whether altered activity in the VAN is associated with LC dysfunction as would be predicted by the adaptive gain theory, we measured associations between pupil dilation during a cognitive task and low frequency BOLD variance (LFBV) during resting-state fMRI. Although the LC can facilitate exploration through high tonic activity, it demonstrates low levels of tonic activity during quiet waking when little vigilance or task-engagement is required (Aston-Jones & Bloom, 1981; Rajkowski, Kubiak, Ivanova, Aston-Jones, 1997; Rajkowski et al., 1994; Rasmussen, Morilak, & Jacobs, 1986). In the context of a resting-state scan with no behavioral demands, the LC should presumably enter a state of low tonic activity with only small fluctuations in activity. Early stages of damage to the LC may result in a paradoxical increase in both LC firing rate and NE metabolism (Chiodo, Acheson, Zigmond, & Stricker, 1983; Elrod et al., 1997; Szot et al., 2006) resulting in a persistent state of high tonic activity. A state of high tonic activity has been proposed to underlie activation of the VAN and sensitivity to environmental stimuli as seen during stimulus-driven states in fMRI

studies of attention (Corbetta et al., 2008). Therefore, higher tonic LC activity may result in greater VAN cortical reactivity, i.e., greater LFBV, due to external stimuli. While low frequency BOLD signal arising from LC activity during resting-state fMRI has been studied in the context of functional connectivity (Bar et al., 2016; Zhang, Hu, Chao, & Li, 2016), we focused on the degree of fluctuation in activity, measured by LFBV, as an index of cortical reactivity brought on by levels of tonic activity.

When functioning normally during cognitive tasks that require focused attention, the LC switches to the phasic mode (Aston-Jones & Cohen, 2005; Nieuwenhuis, Aston-Jones, & Cohen, 2005; Rajkowski, Majczynski, Clayton, & Aston-Jones, 2004). In the event of LC dysfunction, as in preclinical or prodromal AD, the coordinated and temporally specific activity required for phasic responses to behavioral challenges is likely to be impaired (Aston-Jones & Cohen, 2005). The pupil dilation response in the digit span task is well-characterized (Granholm et al., 1996), and we have previously shown that it is sensitive to differences in cognitive status (i.e., MCI) (Granholm et al., 2017). In relation to disrupted LC functioning, a lack of proper phasic modulation may manifest as attenuated (or "flattened") increases in pupil dilation response as task demands increase.

Thus, if early LC dysfunction leads to both a paradoxical increase in tonic LC activity and a reduction in phasic LC activity, as described above, we hypothesized that an association would be found between high levels of LFBV during a resting-state fMRI scan (due to difficulty maintaining low tonic activity) and attenuated increases in pupil dilation response during a digit span task (suggesting inefficient adaptation to changing task demands during phasic state activity).

2. Methods

2.1. Participants

Participants were drawn from wave 2 of the Vietnam Era Twin Study of Aging (VETSA) (Kremen et al., 2006, 2013). VETSA participants comprise a national, community-dwelling male sample that is similar to American men in their age range with respect to health and lifestyle characteristics based on Center for Disease Control and Prevention data (Kremen et al., 2006, 2013; Schoeneborn & Heyman, 2009). The study was approved by the Institutional Review Boards at the University of California, San Diego (UCSD), Boston University (BU), and the Massachusetts General Hospital (MGH). Imaging took place at UCSD and MGH.

Pupillary responses were assessed in 979 individuals at UCSD and BU after excluding participants with a self-reported history of glaucoma in either eye, penetrating eye wounds to both eyes, eye surgery to both eyes that involved the muscle, or use of cholinesterase inhibitors or anticholinergic eye drops. Of these participants, valid pupillary response data were obtained for 954 individuals (in 25 cases data could not be collected due to either technical failure of the equipment or the inability of the subject to complete the task without excessive blinking).

The VETSA 2 MRI component included 447 individuals using standard MRI exclusion criteria (e.g., no metal in the body). Of these, resting-state fMRI (rs-fMRI) data were collected the day after neuropsychological testing and pupillometry sessions on 422 individuals. Forty-four individuals were excluded for excessive motion (mean framewise displacement >.4 mm). The final sample included in the present study was composed of 358 participants with both pupillometry and fMRI data. The sample had a mean age of 61.9 years (SD = 2.65), was primarily Caucasian (89.9%), and had a mean education of 13.8 (SD = 2.06) years. MCI status was determined as described previously in greater detail (Granholm et al., 2017; Kremen et al., 2014) according to the Jak/Bondi actuarial-neuropsychological approach (Bondi et al., 2014; Jak et al., 2009, 2015; Kremen et al., 2014). Thirty individuals were classified as amnestic single domain MCI (aMCI), 15 as non-amnestic single domain MCI (naMCI), and 9 as mMCI.

2.2. Task-evoked pupil dilation

Pupillometry methods have been described previously (Granholm et al., 2017). Briefly, handheld NeurOptics PLR-200 pupillometers were modified by the manufacturer to record pupil diameter from one eye at 30 Hz for up to 15 s in a viewing tube. The device is the size of a television remote with recording optics inside one end of a 1.5-inch viewing tube that surrounds the eye. Ambient light was blocked from reaching the tested eye by the viewing tube; participants closed and held their hand over their other eye.

Pupillary responses were recorded during blocks of trials of 3 (low load), 6 (moderate/near capacity load), and 9 (high/overload) digits presented aurally on a laptop computer at the rate of one per second. Participants heard "Ready" 1 sec before the first digit and "Repeat" 1 sec after the last digit. Each trial was inspected for artifacts in a graphic display on the device. Trials were administered until two clean trials (<50% of data contained artifacts) were recorded or four trials were attempted per digit-span condition. Pupil diameter samples were averaged for each second of recording, which corresponds to the presentation of digits at 1-sec intervals. The primary dependent variable was change relative to baseline during the second immediately following the last digit presented. Baseline pupil size during the first second of each trial was regressed from the pupil change score, to remove individual differences in tonic pupil size.

2.3. Task performance

To determine each individual's short-term memory capacity, we used the maximum span length correctly recalled on the Digit Span subtest of the Wechsler Memory Scale-III (WMS-III; Wechsler, 1997). WMS-III Digit Span was administered prior to digit span trials during pupillometry during the course of neuropsychological testing. Because these data were from wave 2 of the study, we also accounted for practice effects by adjusting wave 2 WMS-III Digit Span scores by the expected increases in scores due to repeated testing. We did not conduct pupillometry in wave 1. As in the study of Ronnlund, Nyberg, Backman, and Nilsson (2005), for each test, we

calculated the difference score as the mean score of participants who underwent cognitive testing at wave 1 minus the mean score of those who took the tests for the first time at wave 2 (attrition replacements). We calculated attrition effects for each test as the mean scores of wave 1 participants who returned for wave 2 minus the mean score of all participants at wave 1. Practice effects were then calculated as the difference score minus the attrition effect. These practice effect values were subtracted from wave 2 scores of returning participants.

2.4. MRI acquisition

Images were acquired at UCSD and MGH. At UCSD, images were acquired with a GE 3T Discovery 750 scanner (GE Healthcare, Waukesha, WI, USA) with an eight-channel phased array head coil. The imaging protocol included a sagittal 3D fast spoiled gradient echo (FSPGR) T_1-weighted volume (TE = 3.164 msec, TR = 8.084 msec, TI = 600 msec, flip angle = 8°, FOV = 256 cm, matrix = 256 × 256, in-plane resolution = 1 × 1 mm, slice thickness = 1.2 mm, slices = 172) used for registration purposes and to determine cortical thickness and surface area. Rs-fMRI scans were collected with a T_2^*-weighted echo-planar imaging sequence (EPI; TE = 30 msec, TR = 3000 msec, flip angle = 85°, FOV = 256, matrix = 64 × 64, in-plane resolution = 4 × 4 mm, slice thickness = 3 mm). Thirty-two slices were acquired in an interleaved order to provide whole-brain coverage. One hundred volumes were acquired (50 forward and 50 reverse phase encoding directions). At MGH, images were acquired with a Siemens Tim Trio, (Siemens USA, Washington, D.C.) with a 32-channel head coil. The imaging protocol included a 3D magnetization-prepared rapid gradient-echo (MPRAGE) T_1-weighted volume (TE = 4.33 msec, TR = 2170 msec, TI = 1100 msec, flip angle = 7°, FOV = 256, matrix = 256 × 256, in-plane resolution = 1 × 1 mm, slice thickness = 1.2 mm, slices = 160). Rs-fMRI scans were collected with a T_2^*-weighted echo-planar imaging sequence (TE = 30 msec, TR = 3000 msec, flip angle = 85°, FOV = 216, matrix = 72 × 72, in-plane resolution = 3 × 3mm, slice thickness = 3 mm). Forty-seven slices were acquired in an interleaved order to provide whole-brain coverage. One-hundred twenty-four volumes were collected.

2.5. MRI processing

Structural MRI images were processed to account for effects of partial voluming on measures of LFBV and to generate anatomical regions of interest (ROIs). The processing methods have been described previously (Kremen et al., 2010; McEvoy et al., 2015) and were based on the FreeSurfer 5.1 software package (Dale, Fischl, & Sereno, 1999; Fischl & Dale, 2000; Fischl, Sereno, & Dale, 1999; Fischl et al., 2004). Surface models were reviewed for accuracy, and white matter and brain masks were manually edited as necessary, in alignment with standard, objective editing rules. The surface was then divided into 66 distinct cortical regions (33 per hemisphere) according to the Desikan-Killiany atlas (Desikan et al., 2006; Fischl et al., 2004). Cortical thickness was extracted from each ROI and standardized with a z-transform.

Rs-fMRI scans were processed as follows: The first 4 volumes were discarded to allow for equilibration of the T_1-weighted signal. B_0 distortions were corrected using the reversing gradient method (Chang & Fitzpatrick, 1992; Holland, Kuperman, & Dale, 2010; Morgan, Bowtell, McIntyre, & Worthington, 2004) and gradient nonlinearity distortions were corrected for each frame (Jovicich et al., 2006). Slice timing correction and motion correction was performed using AFNI (Cox, 1996), and the resulting head motion time courses were later used to regress out motion-related signal. Mean framewise displacement was calculated (Power, Barnes, Snyder, Schlaggar, & Petersen, 2012; Van Dijk, Sabuncu, & Buckner, 2012) for later use as a covariate in group analyses (Satterthwaite et al., 2012). Automated registration between functional and structural images was performed using mutual information (Wells, Viola, Atsumi, Nakajima, & Kikinis, 1996) with coarse pre-alignment based on within-modality registration to atlas brains. Rs-fMRI time courses were normalized with the mean of each voxel. Linear regression was used to remove quadratic trends, motion parameter timecourses, cerebral white matter and whole brain signals, and their first derivatives. Time courses were band-pass filtered between .01 and .08 Hz. We then sampled the time courses at a fixed distance of 1 mm from the white–gray boundary (into the gray matter) onto the cortical surface for each individual subject. The average time course was calculated for each cortical surface-based ROI. Based on our *a priori* hypothesis of key brain regions belonging to the LC-NE system (i.e., TPJ, ACC, and iPFC), we examined LFBV in the supramarginal gyrus (SMG), caudal ACC, and pars opercularis (PO; in the iPFC) ROIs defined by the Desikan-Killiany cortical parcellation (Desikan et al., 2006), respectively. As a negative control, we also assessed the lingual gyrus (LG), a region not particularly associated with the LC-NE system. We did not examine functional connectivity between nodes because we were primarily interested in how the LC modulates activity in each of these regions individually, and LFBV provides an index of fluctuating activity in the tonic state.

2.6. Statistical analysis

Analyses were conducted using linear mixed effects models in R v3.2.1 (R Core Team, 2014). Subjects nested within twin pair were included as random effects to control for repeated measures within subject and correlations within dyads. Differences in pupil dilation were assessed across repeated measures of load (3, 6, or 9 digits). Separate models were run for each hypothesized ROI and the negative control ROI. Task load and LFBV of a given ROI, along with their interaction, were included as fixed effects. To control for differences in task performance, we included the z-transformed maximum forward span (from the WMS-III Digit Span subtest), and its interaction with load as additional fixed effects. The interaction terms of task load with LFBV were of primary interest because they indicate the degree to which change in pupil dilation from one level of task difficulty to another differs as a function of brain activity. Change between levels of load may be more sensitive to LC system disruption than pupil dilation within a given level of load because the former reflects appropriate modulation of activity in response to changing

behavioral contexts. Three models were tested to examine our hypothesized ROI; therefore, the significance threshold was adjusted using a Bonferroni correction ($p < .0167$). Significant associations were determined using the type III test of fixed effects. Where interaction terms were significant, we assessed contrasts of adjacent levels of load to better understand the underlying patterns of change in pupillary response.

We included variables that might be related to either rs-fMRI or pupillary responses. To account for anticholinergic effects of medications not already leading to exclusion on pupillary responses, a composite score reflecting the cumulative anticholinergic effect of all other medications was computed (Granholm et al., 2017). *APOE* genotype was included as a covariate on the basis of presence or absence of an ε4 allele, a risk factor for AD. The standardized cortical thickness of each ROI tested was included to control for effects of atrophy or partial-voluming on functional measures of LFBV. Additional participant-level covariates were included to control for age, pupillometry device (two devices per site), scanner (one per site), handedness (right *vs* left to control for potential differences in lateralization), and mean framewise displacement during the rs-fMRI scan (i.e., motion). The full fixed effects model is shown below; subject nested within case was also included as a random effect to control for non-independence of twin data:

$$PupilDilation_{Load} = Load + LFBV_{ROI} + Load^{*}\ LFBV_{ROI} + MaxForwardSpan + Medication + APOE4 + CortThickness_{ROI} + Age + PupilDevice + Scanner + Handedness + Motion.$$

3. Results

3.1. Participant characteristics and their relationship to LFBV

Only 13 participants were unable to complete 2 trials of all load levels with a clean pupil scan (i.e., with minimal blinks). The average maximum forward span on the WMS-III digit span subtest was 6.86 (SD = 1.89). Maximum digit span was significantly associated with LFBV in the ACC [$t_{(345)} = 2.226$, $p = .027$], but not in either of the other two ROIs. There were 79 (22.07%) *APOE*-ε4 carriers. There were no significant relationships between LFBV and age or *APOE*-ε4 status in any ROIs. LFBV was significantly higher in the SMG in individuals with MCI compared to those who were cognitively normal [$F_{(3,5.19)} = 5.276$, $p = .001$], driven by marginally greater LFBV in aMCI compared to cognitively normal participants [$t_{(335)} = 1.763$, $p = .079$].

3.2. Pupil dilation and LFBV

At any individual level of load (3, 6 or 9), there were no significant relationships between LFBV and pupil dilation for any of the ROIs. However, LFBV was related to the slope of (i.e., change in) pupil dilation across levels of load. After correction for multiple comparisons, there was a significant interaction of LFBV and load on pupil dilation in the SMG [$F_{(2,942)} = 6.959$, $p < .001$], ACC [$F_{(2,942)} = 4.568$, $p = .011$], and PO [$F_{(2,942)} = 8.779$, $p < .001$] (Fig. 1). These interactions were primarily driven by smaller changes in pupil dilation between loads 3 and 6 for participants with higher LFBV [SMG: $t_{(942)} = -2.384$, $p = .017$; ACC: $t_{(942)} = -2.359$, $p = .019$; PO: $t_{(942)} = -2.626$, $p = .009$]. The interaction between LFBV x load was not significant in the negative control region LG [$F_{(2,942)} = .155$, $p = .86$], suggesting a degree of regional specificity in these effects.

3.3. Relationship of pupil dilation with other covariates

The two-way interactions between load x MCI status and load x maximum digit span have been reported previously (Granholm et al., 2017). The three-way interaction of LFBV x load x MCI status was not significant in any ROI, indicating that the interactions between load and pupil dilation reported above did not differ in MCI subjects. No other covariates were significantly related to pupil dilation.

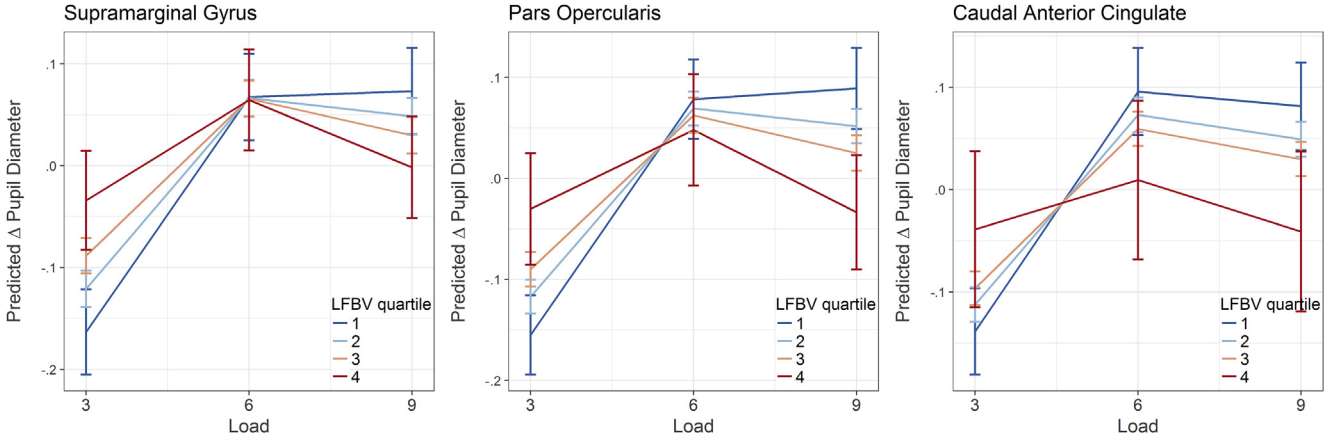

Fig. 1 – Model predicted change in pupil dilation as a function of low frequency BOLD variance (LFBV). Quartiles are shown for ease of interpretation, but LFBV was included as a continuous variable in the models. Error bars represent within-subject standard error. There was a significant interaction ($p < .05$) between load and LFBV in all three regions of interest. This effect was driven by a steeper slope between loads 3 and 6 in individuals with lower LFBV. Note that negative values of change in pupil diameter do not represent constriction, but are a byproduct of mean centering when adjusting for baseline pupil diameter.

4. Discussion

Consistent with our hypotheses, the degree to which pupil responses increase across task loads was related to the variance of rs-fMRI BOLD fluctuations within key nodes of the VAN. We focused on variance in the BOLD signal rather than correlations between regions due to the role of the LC in modulating gain in cortical activity (Aston-Jones & Cohen, 2005). As predicted participants with higher LFBV demonstrated an attenuated increase in pupil dilation between low and moderate levels of task demands (3 and 6 digits), driven by somewhat higher pupil responses at low loads and somewhat lower pupil responses at moderate loads. This flatter pupil dilation slope may reflect two processes, both of which are consistent with less efficient LC function. Slightly greater dilation at the low load may indicate that additional effort is needed to compensate for inefficiency or reduced capacity. However, it does not necessarily mean that people have reached their capacity limit. As seen in Fig. 1, dilation was significantly greater at the moderate load compared with the low load. Instead, the flatter slope associated with higher LFBV suggests that individuals with higher LFBV failed to fully ramp up effort at the moderate load. In effect, they had a narrower dynamic range of response. Put differently, higher LFBV was associated with poorer modulation in response to increasing task demands.

The altered pupillary responses and heightened LFBV is consistent with impaired function of the LC and subsequent NE release. LC dysfunction should result in changes to both tonic and phasic states (Aston-Jones & Cohen, 2005). Level of tonic activity is likely to determine LFBV during the resting-state scan whereas phasic responses likely contribute to pupil dilations during the digit span task (Aston-Jones & Bloom, 1981; Rajkowski et al., 1994, 1997; Rasmussen et al., 1986; Usher, Cohen, Servan-Schreiber, Rajkowski, & Aston-Jones, 1999). Damage to the LC has been shown to result in compensatory increases in LC firing rate and NE metabolism (Chiodo et al., 1983; Elrod et al., 1997; Szot et al., 2006) that may result in a state akin to the tonic mode of LC firing (Aston-Jones & Cohen, 2005; Weinshenker, 2008). In this "persistent tonic state", activity in the VAN may resemble stimulus-driven states of high cortical reactivity in which there are relatively high levels of fluctuating activity that may persist even in situations requiring little vigilance or task engagement such as a resting-state scan.

Our results are consistent with this theory. Higher LFBV may represent increased tonic activity due to LC dysfunction, and a decreased dynamic range in the pupillary response profile during the digit span task may represent a corresponding disruption in phasic activity. During the phasic mode, increased tonic LC firing rate would produce a higher baseline level of activity and individuals may require more effort at low loads. Although phasic activations may still occur, changes in task-related signals are obscured due to a decreased signal-to-noise ratio. That is, the LC shows reduced differentiation in pupil response with increasing task difficulty between low and moderate loads. Consistent with that idea, we previously showed that this reduced differentiation was more severe in more advanced mMCI compared with single-domain MCI (Granholm et al., 2017).

Controlling for maximum digit span means that change in pupillary dilation from low to moderate cognitive loads cannot simply be explained by differences in short-term memory ability. Despite evidence of disrupted LC function, participants with higher LFBV were still able to perform the task successfully, especially at lower loads. This is consistent with the neuromodulatory role of the LC, which facilitates optimal performance and coordinated network functioning by way of NE release through diffuse cortical projections rather than serving as the putative neural substrate of short-term and working memory (Aston-Jones & Cohen, 2005; Coull et al., 1999; Raizada & Poldrack, 2007; Sara, 2009). It may be that even sub-optimal functioning of the LC-NE system and the VAN is sufficient for the digit span task, and performance decrements may only become apparent on more difficult tasks. Alternatively, other compensatory mechanisms may help maintain performance, such as increased cortical sensitivity to NE (Harik et al., 1981; Raskind, Peskind, Holmes, & Goldstein, 1999; Szot et al., 2006, 2007), compensatory reorganization of the LC-NE functional network (Jacobs et al., 2015), or recruitment of additional cortical networks outside of the LC-NE system as is commonly found in fMRI studies of aging and preclinical AD (Cabeza, 2002; Clément & Belleville, 2010; Elman et al., 2014; Huang, Polk, Goh, & Park, 2012; Morcom, Li, & Rugg, 2007; Mormino et al., 2012; Reuter-Lorenz & Cappell, 2008).

A benefit of the relatively narrow age range of the VETSA sample is that the current results are not likely to reflect age-related differences. This is supported by a lack of significant association between age and either pupil dilation or LFBV. Previous research has found age-related *decreases* in BOLD variability, and that greater variability is beneficial (Garrett, Kovacevic, McIntosh, & Grady, 2013, 2010; Grady & Garrett, 2014). The current findings do not necessarily conflict with these reports given the regional specificity of BOLD variability effects observed here and recent findings that BOLD variability demonstrates age-related decreases in some brain regions and increases in others (Nomi, Bolt, Ezie, Uddin, & Heller, 2017). Additionally, there are important differences in the behavioral contexts of fMRI acquisition paradigms between studies that may influence the expected state of LC firing (i.e., fixation blocks interspersed with cognitive tasks *vs* a task-free resting-state scan). In fact, the greater dynamic range in pupil dilation considered to reflect appropriate modulation of LC activity in the current study is consistent with the greater modulation of BOLD variability between behavioral states previously found in young compared to older subjects (Garrett et al., 2013). Thus, it appears that appropriately modulating activity between behavioral contexts is a prime indicator of healthy functioning.

The current study does have several limitations. While we did not have a direct measure of LC activity, a tight link between pupil dilation and LC activity has been shown in humans as well as through single cell recordings in animals (Alnaes et al., 2014; Aston-Jones & Cohen, 2005; Gilzenrat et al., 2010; Joshi et al., 2016; Murphy et al., 2014; Rajkowski et al., 1994, 1993; Samuels & Szabadi, 2008). This link has resulted in the use of pupillometry as a well-validated proxy of mental effort in research over the course of the past few decades (Laeng, Sirois, & Gredebäck, 2012). Further evidence suggests a strong link between activity in the VAN with both pupillary

response and the LC-NE system (Alnaes et al., 2014; Corbetta et al., 2008; Nieuwenhuis, De Geus, & Aston-Jones, 2011; Nieuwenhuis et al., 2005). We based our association between high LFBV and high tonic activity on the proposed link between LC tonic mode and increased sensitivity to environmental stimuli within the VAN (Corbetta et al., 2008). However, the relationship between LC activation and expected BOLD signal in the cortex is complex. Single cell recordings during tonic activation of LC neurons and subsequent release of NE demonstrate that modulatory effects differ on a cell-by-cell basis depending on brain region, frequency and strength of stimulation, and behavioral context (Devilbiss & Waterhouse, 2004, 2011; Polack, Friedman, & Golshani, 2013; Poulet & Petersen, 2008). This is further complicated by the relationship between cortical synchrony with BOLD signal, which can differ by region and frequency band (Conner, Ellmore, Pieters, DiSano, & Tandon, 2011; Winterer et al., 2007). The relationships between pupil dilation and LFBV found in the current study appear to be regionally specific, and thus do not reflect global properties of brain activity. We note that, at least in the SMG, participants with MCI showed higher LFBV, suggesting that higher variability in this region is indicative of disrupted or inefficient functioning. Further work is necessary to elucidate the complex relationship between single-cell recordings of LC activity and resulting cortical BOLD signal.

Similarly, we were not able to directly assess pathology within the LC in these participants. Although there may be multiple factors driving differences in pupil dilation and LFBV, there is reason to suspect that AD-related processes – the presence of abnormal tau in particular – play a role. A study of 2,332 autopsy examinations across all age ranges found AD-related tau inclusions in nearly every case, and there is evidence that the earliest site of abnormal tau is in the LC (Braak & Del Tredici, 2011; Braak, Thal, Ghebremedhin, & Del Tredici, 2011). These findings have been proposed to reflect AD pathological processes that originate in the brainstem and progress across the lifespan (Braak & Del Tredici, 2012; although see; Crary et al., 2014). Although there may be little or no detrimental effects on neural functioning in the initial stages, the LC is likely to be one of the first brain regions affected when conformational changes result in more toxic forms of tau. Evidence that abnormal tau can precipitate formation of Aβ plaques and exacerbate inflammatory responses provides additional avenues through which early LC dysfunction may have downstream effects on cortical functioning (Chalermpalanupap et al., 2013; Heneka et al., 2002, 2010). Therefore, altered activity within the LC may represent both a functional outcome and key contributor to disease progression. However, further work is necessary to determine whether pathology within the LC is specific to AD-related processes.

With the continued development of tau PET tracers, it may soon be feasible to include *in vivo* imaging measures of tau deposits in future studies focusing on the LC. However, the relatively low resolution of PET imaging and off-target binding in the brainstem likely preclude direct measurement of tau within the LC itself. We also do not know which of the current participants may go on to develop AD, but we will be able to examine this in future waves of the study. On the other hand, we did show that pupillary responses differentiated cognitively normal and MCI groups (Granholm et al., 2017), and individuals with MCI tended to have greater LFBV in the current analysis. Lastly, we did not collect task-based fMRI or resting-state pupil dilation recordings. Therefore, we were unable to assess the relationship between patterns of tonic and phasic activity within modality.

We previously found that pupil dilation response differs based on MCI status. The current study suggests that differences in pupil dilation are related to dysfunction in the LC by linking differences in task-evoked pupil responses with cortical activity of regions belonging to the LC-NE system. We propose that these findings reflect the ability to appropriately modulate LC activity given the behavioral context. That is, LC dysfunction likely results in disruptions to both tonic and phasic modes of activity. Recent evidence that abnormal tau is present in the LC much earlier than previously thought suggests that impaired LC functioning may reflect early phase AD-related processes. The relationship between pupillary response and LFBV is consistent with the idea that the effects of any such processes in the LC may be propagated to cortical functioning. That these changes in pupillary response are detectable in the absence of substantial performance decrements suggests that this easily implemented measure of pupillary response may ultimately have utility as a marker of impaired LC functioning and as an additional early screening tool for AD-related risk. However, further work is necessary to determine the specificity of pupil dilation responses in relation to LC dysfunction and AD-related risk. Finally, the results provide a strong rationale for the value of further study of LC integrity in conjunction with fMRI examination of LFBV during cognitive task performance.

Acknowledgements and Disclosures

The content of this manuscript is the responsibility of the authors and does not represent official views of NIA/NIH, or the Veterans' Administration. Numerous organizations provided invaluable assistance in the conduct of the VET Registry, including: U.S. Department of Veterans Affairs, Department of Defense; National Personnel Records Center, National Archives and Records Administration; Internal Revenue Service; National Opinion Research Center; National Research Council, National Academy of Sciences; the Institute for Survey Research, Temple University. The authors gratefully acknowledge the continued cooperation of the twins and the efforts of many staff members. The study was supported by awards from the National Institutes of Health/National Institute on Aging [R01s AG018386, AG022381, AG022982, AG050595 to W.S.K.; R01 AG018384 to M.J.L.; R03 AG 046413 to C.E.F, and K08 AG047903 to M.S.P].

L.K. McEvoy has stock options in CorTechs Laboratories, Inc. A.M. Dale is a Founder of and holds equity in CorTechs Laboratories, Inc, and serves on its Scientific Advisory Board. He is a member of the Scientific Advisory Board of Human Longevity, Inc and receives funding through research agreements with General Electric Healthcare and Medtronic, Inc. The terms of these arrangements have been reviewed and approved by University of California, San Diego in accordance

with its conflict of interest policies. The other authors report no conflicts.

REFERENCES

Aizenstein, H. J., Nebes, R. D., Saxton, J. A., Price, J. C., Mathis, C. A., Tsopelas, N. D., et al. (2008). Frequent amyloid deposition without significant cognitive impairment among the elderly. *Archives of Neurology, 65*, 1509–1517.

Alnaes, D., Sneve, M. H., Espeseth, T., Endestad, T., van de Pavert, S. H., & Laeng, B. (2014). Pupil size signals mental effort deployed during multiple object tracking and predicts brain activity in the dorsal attention network and the locus coeruleus. *Journal of Vision, 14*.

Aston-Jones, G., & Bloom, F. E. (1981). Activity of norepinephrine-containing locus coeruleus neurons in behaving rats anticipates fluctuations in the sleep-waking cycle. *The Journal of Neuroscience, 1*, 876–886.

Aston-Jones, G., & Cohen, J. D. (2005). An integrative theory of locus coeruleus-norepinephrine function: Adaptive gain and optimal performance. *Annual Review of Neuroscience, 28*, 403–450.

Aston-Jones, G., Rajkowski, J., Lu, W., Zhu, Y., Cohen, J. D., & Morecraft, R. J. (2002). Prominent projections from the orbital prefrontal cortex to the locus coeruleus in monkey. *Society for Neuroscience Abstracts*, 86–89.

Bar, K. J., de la Cruz, F., Schumann, A., Koehler, S., Sauer, H., Critchley, H., et al. (2016). Functional connectivity and network analysis of midbrain and brainstem nuclei. *NeuroImage, 134*, 53–63.

Bateman, R. J., Xiong, C., Benzinger, T. L., Fagan, A. M., Goate, A., Fox, N. C., et al. (2012). Clinical and biomarker changes in dominantly inherited Alzheimer's disease. *The New England Journal of Medicine, 367*, 795–804.

Bennett, D. A., Schneider, J. A., Arvanitakis, Z., Kelly, J. F., Aggarwal, N. T., Shah, R. C., et al. (2006). Neuropathology of older persons without cognitive impairment from two community-based studies. *Neurology, 66*, 1837–1844.

Bondareff, W., Mountjoy, C. Q., Roth, M., Rossor, M. N., Iversen, L. L., Reynolds, G. P., et al. (1987). Neuronal degeneration in locus ceruleus and cortical correlates of Alzheimer disease. *Alzheimer Disease and Associated Disorders, 1*, 256–262.

Bondi, M. W., Edmonds, E. C., Jak, A. J., Clark, L. R., Delano-Wood, L., McDonald, C. R., et al. (2014). Neuropsychological criteria for mild cognitive impairment improves diagnostic precision, biomarker associations, and progression rates. *Journal of Alzheimers Disease, 42*(1), 275–289. https://doi.org/10.3233/JAD-140276.

Braak, H., & Del Tredici, K. (2011). The pathological process underlying Alzheimer's disease in individuals under thirty. *Acta Neuropathologica, 121*, 171–181.

Braak, H., & Del Tredici, K. (2012). Where, when, and in what form does sporadic Alzheimer's disease begin? *Current Opinion in Neurology, 25*, 708–714.

Braak, H., Thal, D. R., Ghebremedhin, E., & Del Tredici, K. (2011). Stages of the pathologic process in Alzheimer disease: Age categories from 1 to 100 years. *Journal of Neuropathology and Experimental Neurology, 70*, 960–969.

Cabeza, R. (2002). Hemispheric asymmetry reduction in older adults: The HAROLD model. *Psychology and Aging, 17*, 85–100.

Chalermpalanupap, T., Kinkead, B., Hu, W. T., Kummer, M. P., Hammerschmidt, T., Heneka, M. T., et al. (2013). Targeting norepinephrine in mild cognitive impairment and Alzheimer's disease. *Alzheimer's Research & Therapy, 5*, 21.

Chang, H., & Fitzpatrick, J. M. (1992). A technique for accurate magnetic resonance imaging in the presence of field inhomogeneities. *IEEE Transactions on Medical Imaging, 11*, 319–329.

Chiodo, L. A., Acheson, A. L., Zigmond, M. J., & Stricker, E. M. (1983). Subtotal destruction of central noradrenergic projections increases the firing rate of locus coeruleus cells. *Brain Research, 264*, 123–126.

Clément, F., & Belleville, S. (2010). Compensation and disease severity on the memory-related activations in mild cognitive impairment. *Biological Psychiatry, 68*, 894–902.

Conner, C. R., Ellmore, T. M., Pieters, T. A., DiSano, M. A., & Tandon, N. (2011). Variability of the relationship between electrophysiology and BOLD-fMRI across cortical regions in humans. *The Journal of Neuroscience, 31*, 12855–12865.

Corbetta, M., Patel, G., & Shulman, G. L. (2008). The reorienting system of the human brain: From environment to theory of mind. *Neuron, 58*, 306–324.

Coull, J. T., Büchel, C., Friston, K. J., & Frith, C. D. (1999). Noradrenergically mediated plasticity in a human attentional neuronal network. *NeuroImage, 10*, 705–715.

Cox, R. W. (1996). AFNI: Software for analysis and visualization of functional magnetic resonance neuroimages. *Computers and Biomedical Research, 29*, 162–173.

Crary, J. F., Trojanowski, J. Q., Schneider, J. A., Abisambra, J. F., Abner, E. L., Alafuzoff, I., et al. (2014). Primary age-related tauopathy (PART): A common pathology associated with human aging. *Acta Neuropathologica, 128*, 755–766.

Dale, A. M., Fischl, B., & Sereno, M. I. (1999). Cortical surface-based analysis. I. Segmentation and surface reconstruction. *NeuroImage, 9*, 179–194.

Desikan, R. S., Segonne, F., Fischl, B., Quinn, B. T., Dickerson, B. C., Blacker, D., et al. (2006). An automated labeling system for subdividing the human cerebral cortex on MRI scans into gyral based regions of interest. *NeuroImage, 31*, 968–980.

Devilbiss, D. M., & Waterhouse, B. D. (2004). The effects of tonic locus ceruleus output on sensory-evoked responses of ventral posterior medial thalamic and barrel field cortical neurons in the awake rat. *The Journal of Neuroscience, 24*, 10773–10785.

Devilbiss, D. M., & Waterhouse, B. D. (2011). Phasic and tonic patterns of locus coeruleus output differentially modulate sensory network function in the awake rat. *Journal of Neurophysiology, 105*, 69–87.

Dosenbach, N. U. F., Visscher, K. M., Palmer, E. D., Miezin, F. M., Wenger, K. K., Kang, H. C., et al. (2006). A core system for the implementation of task sets. *Neuron, 50*, 799–812.

Dubois, B., Feldman, H. H., Jacova, C., Hampel, H., Molinuevo, J. L., Blennow, K., et al. (2014). Advancing research diagnostic criteria for Alzheimer's disease: The IWG-2 criteria. *Lancet Neurology, 13*, 614–629.

Elman, J. A., Oh, H., Madison, C. M., Baker, S. L., Vogel, J. W., Marks, S. M., et al. (2014). Neural compensation in older people with brain amyloid-beta deposition. *Nature Neuroscience, 17*, 1316–1318.

Elrod, R., Peskind, E. R., DiGiacomo, L., Brodkin, K. I., Veith, R. C., & Raskind, M. A. (1997). Effects of Alzheimer's disease severity on cerebrospinal fluid norepinephrine concentration. *The American Journal of Psychiatry, 154*, 25–30.

Ewers, M., Sperling, R. A., Klunk, W. E., Weiner, M. W., & Hampel, H. (2011). Neuroimaging markers for the prediction and early diagnosis of Alzheimer's disease dementia. *Trends in Neurosciences, 34*, 430–442.

Fischl, B., & Dale, A. M. (2000). Measuring the thickness of the human cerebral cortex from magnetic resonance images. *Proceedings of the National Academy of Sciences of the United States of America, 97*, 11050–11055.

Fischl, B., Sereno, M. I., & Dale, A. M. (1999). Cortical surface-based analysis. II: Inflation, flattening, and a surface-based coordinate system. *NeuroImage, 9*, 195–207.

Fischl, B., van der Kouwe, A., Destrieux, C., Halgren, E., Segonne, F., Salat, D. H., et al. (2004). Automatically parcellating the human cerebral cortex. *Cerebral Cortex, 14*, 11–22.

Garrett, D. D., Kovacevic, N., McIntosh, A. R., & Grady, C. L. (2010). Blood oxygen level-dependent signal variability is more than just noise. *The Journal of Neuroscience, 30*, 4914–4921.

Garrett, D. D., Kovacevic, N., McIntosh, A. R., & Grady, C. L. (2013). The modulation of BOLD variability between cognitive states varies by age and processing speed. *Cerebral Cortex, 23*, 684–693.

German, D. C., Manaye, K. F., White, C. L., Woodward, D. J., McIntire, D. D., Smith, W. K., et al. (1992). Disease-specific patterns of locus coeruleus cell loss. *Annals of Neurology, 32*, 667–676.

German, D. C., White, C. L., & Sparkman, D. R. (1987). Alzheimer's disease: Neurofibrillary tangles in nuclei that project to the cerebral cortex. *Neuroscience, 21*, 305–312.

Geva, R., Zivan, M., Warsha, A., & Olchik, D. (2013). Alerting, orienting or executive attention networks: Differential patters of pupil dilations. *Frontiers in Behavioral Neuroscience, 7*.

Gilzenrat, M. S., Nieuwenhuis, S., Jepma, M., & Cohen, J. D. (2010). Pupil diameter tracks changes in control state predicted by the adaptive gain theory of locus coeruleus function. *Cognitive, Affective, & Behavioral Neuroscience, 10*, 252–269.

Golde, T. E., Schneider, L. S., & Koo, E. H. (2011). Anti-abeta therapeutics in Alzheimer's disease: The need for a paradigm shift. *Neuron, 69*, 203–213.

Grady, C. L., & Garrett, D. D. (2014). Understanding variability in the BOLD signal and why it matters for aging. *Brain Imaging and Behavior, 8*, 274–283.

Granholm, E., Asarnow, R. F., Sarkin, A. J., & Dykes, K. L. (1996). Pupillary responses index cognitive resource limitations. *Psychophysiology, 33*, 457–461.

Granholm, E. L., Panizzon, M. S., Elman, J. A., Jak, A. J., Hauger, R. L., Bondi, M. W., et al. (2017). Pupillary responses as a biomarker of early risk for Alzheimer's disease. *Journal of Alzheimers Disease, 56*, 1419–1428.

Grudzien, A., Shaw, P., Weintraub, S., Bigio, E., Mash, D. C., & Mesulam, M. M. (2007). Locus coeruleus neurofibrillary degeneration in aging, mild cognitive impairment and early Alzheimer's disease. *Neurobiology of Aging, 28*, 327–335.

Harik, S., Duckrow, R., LaManna, J., Rosenthal, M., Sharma, V., & Banerjee, S. (1981). Cerebral compensation for chronic noradrenergic denervation induced by locus ceruleus lesion: Recovery of receptor binding, isoproterenol- induced adenylate cyclase activity, and oxidative metabolism. *The Journal of Neuroscience, 1*, 641–649.

Heneka, M. T., Galea, E., Gavriluyk, V., Dumitrescu-Ozimek, L., Daeschner, J., O'Banion, M. K., et al. (2002). Noradrenergic depletion potentiates beta-amyloid-induced cortical inflammation: Implications for Alzheimer's disease. *The Journal of Neuroscience, 22*, 2434–2442.

Heneka, M. T., Nadrigny, F., Regen, T., Martinez-Hernandez, A., Dumitrescu-Ozimek, L., Terwel, D., et al. (2010). Locus ceruleus controls Alzheimer's disease pathology by modulating microglial functions through norepinephrine. *Proceedings of the National Academy of Sciences of the United States of America, 107*, 6058–6063.

Holland, D., Kuperman, J. M., & Dale, A. M. (2010). Efficient correction of inhomogeneous static magnetic field-induced distortion in Echo Planar Imaging. *NeuroImage, 50*, 175–183.

Huang, C.-M., Polk, T. A., Goh, J. O., & Park, D. C. (2012). Both left and right posterior parietal activations contribute to compensatory processes in normal aging. *Neuropsychologia, 50*, 55–66.

Jacobs, H. I. L., Wiese, S., van de Ven, V., Gronenschild, E. H. B. M., Verhey, F. R. J., & Matthews, P. M. (2015). Relevance of parahippocampal-locus coeruleus connectivity to memory in early dementia. *Neurobiology of Aging, 36*, 618–626.

Jak, A. J., Bondi, M. W., Delano-Wood, L., Wierenga, C., Corey-Bloom, J., Salmon, D. P., et al. (2009). Quantification of five neuropsychological approaches to defining mild cognitive impairment. *American Journal of Geriatric Psychiatry, 17*, 368–375.

Jak, A. J., Panizzon, M. S., Spoon, K. M., Fennema-Notestine, C., Franz, C. E., Thompson, W. K., et al. (2015). Hippocampal atrophy varies by neuropsychologically defined MCI among men in their 50s. *The American Journal of Geriatric Psychiatry, 23*, 456–465.

Jansen, W. J., Ossenkoppele, R., Knol, D. L., Tijms, B. M., Scheltens, P., Verhey, F. R., et al. (2015). Prevalence of cerebral amyloid pathology in persons without dementia: A meta-analysis. *JAMA, 313*, 1924–1938.

Joshi, S., Li, Y., Kalwani, R. M., & Gold, J. I. (2016). Relationships between pupil diameter and neuronal activity in the locus coeruleus, colliculi, and cingulate cortex. *Neuron, 89*, 221–234.

Jovicich, J., Czanner, S., Greve, D., Haley, E., van der Kouwe, A., Gollub, R., et al. (2006). Reliability in multi-site structural MRI studies: Effects of gradient non-linearity correction on phantom and human data. *NeuroImage, 30*, 436–443.

Koss, M. C. (1986). Pupillary dilation as an index of central nervous system alpha 2-adrenoceptor activation. *Journal of Pharmacological Methods, 15*, 1–19.

Kremen, W. S., Franz, C. E., & Lyons, M. J. (2013). VETSA: The Vietnam Era twin study of aging. *Twin Research and Human Genetics, 16*, 399–402.

Kremen, W. S., Jak, A. J., Panizzon, M. S., Spoon, K. M., Franz, C. E., Thompson, W. K., et al. (2014). Early identification and heritability of mild cognitive impairment. *International Journal of Epidemiology, 43*, 600–610.

Kremen, W. S., Prom-Wormley, E., Panizzon, M. S., Eyler, L. T., Fischl, B., Neale, M. C., et al. (2010). Genetic and environmental influences on the size of specific brain regions in midlife: The VETSA MRI study. *NeuroImage, 49*, 1213–1223.

Kremen, W. S., Thompson-Brenner, H., Leung, Y. M., Grant, M. D., Franz, C. E., Eisen, S. A., et al. (2006). Genes, environment, and time: The Vietnam Era twin study of aging (VETSA). *Twin Research and Human Genetics, 9*, 1009–1022.

Laeng, B., Sirois, S., & Gredebäck, G. (2012). Pupillometry a window to the preconscious? *Perspectives on Psychological Science, 7*, 18–27.

McEvoy, L. K., Fennema-Notestine, C., Eyler, L. T., Franz, C. E., Hagler, D. J., Jr., Lyons, M. J., et al. (2015). Hypertension-related alterations in white matter microstructure detectable in middle age. *Hypertension, 66*, 317–323.

Morcom, A. M., Li, J., & Rugg, M. D. (2007). Age effects on the neural correlates of episodic Retrieval: Increased cortical recruitment with matched performance. *Cerebral Cortex, 17*, 2491–2506.

Morgan, P. S., Bowtell, R. W., McIntyre, D. J., & Worthington, B. S. (2004). Correction of spatial distortion in EPI due to inhomogeneous static magnetic fields using the reversed gradient method. *Journal of Magnetic Resonance Imaging, 19*, 499–507.

Mormino, E. C., Brandel, M. G., Madison, C. M., Marks, S., Baker, S. L., & Jagust, W. J. (2012). Aβ deposition in aging is associated with increases in brain activation during successful memory encoding. *Cerebral Cortex, 22*, 1813–1823.

Murphy, P. R., O'Connell, R. G., O'Sullivan, M., Robertson, I. H., & Balsters, J. H. (2014). Pupil diameter covaries with BOLD activity in human locus coeruleus: Pupil diameter and locus coeruleus activity. *Human Brain Mapping, 35*, 4140–4154.

Nieuwenhuis, S., Aston-Jones, G., & Cohen, J. D. (2005). Decision making, the P3, and the locus coeruleus-norepinephrine system. *Psychological Bulletin, 131*, 510–532.

Nieuwenhuis, S., De Geus, E. J., & Aston-Jones, G. (2011). The anatomical and functional relationship between the P3 and autonomic components of the orienting response. *Psychophysiology, 48*, 162–175.
Nomi, J. S., Bolt, T. S., Ezie, C. E. C., Uddin, L. Q., & Heller, A. S. (2017). Moment-to-Moment BOLD signal variability reflects regional changes in neural flexibility across the lifespan. *The Journal of Neuroscience, 37*, 5539–5548.
Polack, P. O., Friedman, J., & Golshani, P. (2013). Cellular mechanisms of brain state-dependent gain modulation in visual cortex. *Nature Neuroscience, 16*, 1331–1339.
Poulet, J. F., & Petersen, C. C. (2008). Internal brain state regulates membrane potential synchrony in barrel cortex of behaving mice. *Nature, 454*, 881–885.
Power, J. D., Barnes, K. A., Snyder, A. Z., Schlaggar, B. L., & Petersen, S. E. (2012). Spurious but systematic correlations in functional connectivity MRI networks arise from subject motion. *NeuroImage, 59*, 2142–2154.
R Core Team. (2014). *R: A language and environment for statistical computing*. Vienna, Austria: R Foundation for Statistical Computing, 2012. ISBN 3-900051-07-0.
Raizada, R. D., & Poldrack, R. A. (2007). Challenge-driven attention: Interacting frontal and brainstem systems. *Frontiers in Human Neuroscience, 1*, 3.
Rajkowski, J., Kubiak, P., & Aston-Jones, G. (1993). Correlations between locus coeruleus (LC) neural activity, pupil diameter and behavior in monkey support a role of LC in attention. *Society for Neuroscience Abstracts, 19*, 974.
Rajkowski, J., Kubiak, P., & Aston-Jones, G. (1994). Locus coeruleus activity in monkey: Phasic and tonic changes are associated with altered vigilance. *Brain Research Bulletin, 35*, 607–616.
Rajkowski, J., Kubiak, P., Ivanova, S., & Aston-Jones, G. (1997). State-related activity, reactivity of locus ceruleus neurons in behaving monkeys. In S. David, G. E. Goldstein, & M. Richard (Eds.), *Advances in pharmacology* (pp. 740–744). Academic Press.
Rajkowski, J., Majczynski, H., Clayton, E., & Aston-Jones, G. (2004). Activation of monkey locus coeruleus neurons varies with difficulty and performance in a target detection task. *Journal of Neurophysiology, 92*, 361–371.
Raskind, M. A., Peskind, E. R., Holmes, C., & Goldstein, D. S. (1999). Patterns of cerebrospinal fluid catechols support increased central noradrenergic responsiveness in aging and Alzheimer's disease. *Biological Psychiatry, 46*, 756–765.
Rasmussen, K., Morilak, D. A., & Jacobs, B. L. (1986). Single unit activity of locus coeruleus neurons in the freely moving cat. I. During naturalistic behaviors and in response to simple and complex stimuli. *Brain Research, 371*, 324–334.
Reuter-Lorenz, P. A., & Cappell, K. A. (2008). Neurocognitive aging and the compensation hypothesis. *Current Directions in Psychological Science, 17*, 177–182.
Ronnlund, M., Nyberg, L., Backman, L., & Nilsson, L. G. (2005). Stability, growth, and decline in adult life span development of declarative memory: Cross-sectional and longitudinal data from a population-based study. *Psychology and Aging, 20*, 3–18.
Samuels, E. R., & Szabadi, E. (2008). Functional neuroanatomy of the noradrenergic locus coeruleus: Its roles in the regulation of arousal and autonomic function Part II: Physiological and pharmacological manipulations and pathological alterations of locus coeruleus activity in humans. *Current Neuropharmacology, 6*, 254–285.
Sara, S. J. (2009). The locus coeruleus and noradrenergic modulation of cognition. *Nature Reviews Neuroscience, 10*, 211–223.
Sara, S. J., & Bouret, S. (2012). Orienting and reorienting: The locus coeruleus mediates cognition through arousal. *Neuron, 76*, 130–141.
Satterthwaite, T. D., Wolf, D. H., Loughead, J., Ruparel, K., Elliott, M. A., Hakonarson, H., et al. (2012). Impact of in-scanner head motion on multiple measures of functional connectivity: Relevance for studies of neurodevelopment in youth. *NeuroImage, 60*, 623–632.
Schoeneborn, C. A., & Heyman, K. M. (2009). *Health characteristics of adults aged 55 years and over: United States, 2004-2007. National health statistics reports; no. 16. National health statistics reports.* Hyattsville, MD: National Center for Health Statistics.
Sperling, R. A., Aisen, P. S., Beckett, L. A., Bennett, D. A., Craft, S., Fagan, A. M., et al. (2011). Toward defining the preclinical stages of Alzheimer's disease: Recommendations from the national Institute on aging-Alzheimer's association workgroups on diagnostic guidelines for Alzheimer's disease. *Alzheimer's & Dementia, 7*, 280–292.
Szot, P., White, S. S., Greenup, J. L., Leverenz, J. B., Peskind, E. R., & Raskind, M. A. (2006). Compensatory changes in the noradrenergic nervous system in the locus ceruleus and hippocampus of postmortem subjects with Alzheimer's disease and dementia with lewy bodies. *The Journal of Neuroscience, 26*, 467–478.
Szot, P., White, S. S., Greenup, J. L., Leverenz, J. B., Peskind, E. R., & Raskind, M. A. (2007). Changes in adrenoreceptors in the prefrontal cortex of subjects with dementia: Evidence of compensatory changes. *Neuroscience, 146*, 471–480.
Usher, M., Cohen, J. D., Servan-Schreiber, D., Rajkowski, J., & Aston-Jones, G. (1999). The role of locus coeruleus in the regulation of cognitive performance. *Science, 283*, 549–554.
Van Dijk, K. R. A., Sabuncu, M. R., & Buckner, R. L. (2012). The influence of head motion on intrinsic functional connectivity MRI. *NeuroImage, 59*, 431–438.
Varazzani, C., San-Galli, A., Gilardeau, S., & Bouret, S. (2015). Noradrenaline and dopamine neurons in the reward/effort trade-off: A direct electrophysiological comparison in behaving monkeys. *The Journal of neuroscience, 35*, 7866–7877.
Walz, J. M., Goldman, R. I., Carapezza, M., Muraskin, J., Brown, T. R., & Sajda, P. (2013). Simultaneous EEG-fMRI reveals temporal evolution of coupling between supramodal cortical attention networks and the brainstem. *The Journal of Neuroscience, 33*, 19212–19222.
Wechsler, D. (1997). *Wechsler adult intelligence scale-III (WAIS-III) manual*. San Antonio, TX: The Psychological Corporation.
Weinshenker, D. (2008). Functional consequences of locus coeruleus degeneration in Alzheimer's disease. *Current Alzheimer Research, 5*, 342–345.
Wells, W. M., 3rd, Viola, P., Atsumi, H., Nakajima, S., & Kikinis, R. (1996). Multi-modal volume registration by maximization of mutual information. *Medical Image Analysis, 1*, 35–51.
Winterer, G., Carver, F. W., Musso, F., Mattay, V., Weinberger, D. R., & Coppola, R. (2007). Complex relationship between BOLD signal and synchronization/desynchronization of human brain MEG oscillations. *Human Brain Mapping, 28*, 805–816.
Zhang, S., Hu, S., Chao, H. H., & Li, C. S. (2016). Resting-state functional connectivity of the locus coeruleus in Humans: In comparison with the ventral tegmental area/substantia nigra pars compacta and the effects of age. *Cerebral Cortex, 26*, 3413–3427.